
A Pseudo-Metric between Probability Distributions based on Depth-Trimmed Regions

Guillaume Staerman, Pavlo Mozharovskyi, Stéphan Cléménçon, Florence d’Alché-Buc
 LTCI, Télécom Paris, Institut Polytechnique de Paris
 name.surname@telecom-paris.fr

Abstract

The design of a metric between probability distributions is a longstanding problem motivated by numerous applications in Machine Learning. Focusing on continuous probability distributions on the Euclidean space \mathbb{R}^d , we introduce a novel pseudo-metric between probability distributions by leveraging the extension of univariate quantiles to multivariate spaces. Data depth is a nonparametric statistical tool that measures the centrality of any element $x \in \mathbb{R}^d$ with respect to (w.r.t.) a probability distribution or a data set. It is a natural median-oriented extension of the cumulative distribution function (cdf) to the multivariate case. Thus, its upper level sets—the depth-trimmed regions—give rise to a definition of multivariate quantiles. The new pseudo-metric relies on the average of the Hausdorff distance between the depth-based quantile regions w.r.t. each distribution. After discussing the properties of this pseudo-metric inherited from data depth, we provide conditions under which it defines a distance. Interestingly, the derived non-asymptotic bound shows that in contrast to the widely used Wasserstein distance, the proposed pseudo-metric does not suffer from the curse of dimensionality. Robustness, an appealing feature of this pseudo-metric, is studied through the finite sample breakdown point. Moreover, we propose an efficient approximation method with linear time complexity w.r.t. the size of the data set and its dimension. The quality of this approximation as well as the performance of the proposed approach are illustrated in numerical experiments.

1 Introduction

Metrics or pseudo-metrics between probability distributions have attracted a long-standing interest in information theory [1, 2, 3, 4], probability theory and statistics [5, 6, 7, 8]. While they serve many purposes in machine learning [9, 10], they are of crucial importance as loss functions in generative modeling [11] whether it be adversarial [12] or not, as well as in variational inference [13]. Yet designing a measure to compare two probability distributions is considered as a challenging research field. This is certainly due to the inherent difficulty to capture in a single measure typical desired properties such as: (i) metric or pseudo metric properties, (ii) invariance under specific geometric transformations, (iii) convergence and (iv) non-asymptotic bounds on this measure between a sample and its generating law, and eventually, (v) efficient computation on data sets. The f -divergences among which the Kullback-Leibler (KL) divergence is the most popular, the Integral Probability Metrics (IPM) and Optimal Transport Distances are only a few examples of the large collection of discrepancies between probability distributions introduced in the literature. Although the L_1 -Wassertein distance belongs to the two latter classes both at the same time, these (pseudo-) metrics rely on different principles.

The f -divergences [2] are defined as the weighted average by a well-chosen function f of the odds ratio between the two distributions. They are widely used in statistical inference but they are by design ill-defined when the supports of both distributions do not overlap, which appears to be a

crucial limitation in many applications. IPMs are based on a variational definition of the metric, *i.e.* the maximum difference in expectation for both distributions calculated over a class of measurable functions and give rise to various metrics (Maximum Mean Discrepancy (MMD), Dudley's metric, L_1 -Wasserstein Distance) depending on the choice of this class. However, except the case of MMD which appears to enjoy a closed-form solution, the variational definition raises issues in computation. From the side of Optimal transport (OT) [14, 15], the L_p -Wasserstein distance [16] is based on a ground metric able to take into account the geometry of the space on which the distributions are defined. Its ability to deal with non-overlapping support as well as its appealing theoretical properties make OT a powerful tool, particularly when applied to generative models [17] or domain adaptation [18]. However, the Wasserstein distance suffers from two major difficulties: (i) the curse of dimensionality with convergence rates of order $O(n^{-1/d})$ where n is the sample size [19] and (ii) its computational cost as it requires $O(n^3)$ operations. To overcome this computational challenge, many techniques relying upon entropic regularization [20, 21], or one-dimensional projections like the Sliced-Wasserstein distance [22, 23], have been introduced.

In this work we adopt a different point of view. Focusing on continuous probability distributions on the Euclidean space \mathbb{R}^d , we propose to consider a new metric between probability distributions by leveraging the extension of univariate quantiles to multivariate spaces. The notion of quantile function stands as an interesting ground to build a comparison between two probability measures as illustrated by the closed-form of the Wasserstein distance defined over \mathbb{R} . However, given the lack of natural ordering on \mathbb{R}^d as soon as $d > 1$, extending the concept of univariate quantiles to the multivariate case raises a real challenge. Many extensions have been proposed in the literature such as Minimum Volume Sets [24], spatial quantiles [25] or data depth [26]. The latter offers different ways of ordering multivariate data w.r.t a probability distribution. Precisely, *data depths* are non parametric statistics that determine the centrality of any element $x \in \mathbb{R}^d$ w.r.t. a probability measure. They provide a multivariate ordering based on topological properties of the distribution allowing it to be characterized by its location, scale or shape (see *e.g.* [27] for a review). Several data depths were subsequently proposed such as convex hull peeling depth [28], simplicial depth [29], Oja depth [30] or zonoid depth [31] differing in their properties and applications. With a substantial body of literature devoted to its computation, recent advances allow for fast exact [32] and approximate [33] computation of several depth notions. The desirable properties of data depth such as affine invariance, continuity w.r.t. its arguments, and robustness [34] make it an important tool in many fields. Today, in its variety of notions and applications, data depth constitutes a versatile methodology [35] that has been successfully employed in a variety of machine learning tasks among which regression [36, 37], classification [38, 39], anomaly detection [40, 41, 42, 43] and clustering [44].

This paper presents a new discrepancy measure between probability distributions, well-defined for non-overlapping supports, that leverages the interesting features of data depths. This measure is studied at the lens of the properties we stated previously, yielding the contributions listed below.

Contributions:

- A new discrepancy measure between probability distributions involving the upper-level sets of data depth is introduced. We show that this measure is a pseudo-metric in general and exhibit situations where it defines a distance. Its good behavior w.r.t. major transformation groups is depicted. Its ability to factor out translations is also being studied.
- Given empirical distributions, conditions under which strong consistency for the built estimator is respected are put forward. Convergence rate, which does not suffer from the curse of dimensionality remarkably, is provided when the discrepancy is associated with the halfspace depth. The finite sample breakdown point of the proposed distance is also investigated to illustrate the robustness of the proposed discrepancy measure.
- An efficient approximation of the depth-trimmed regions based pseudo-metric is proposed for halfspace and projection depths. It relies on a nice feature of the Hausdorff distance when computed between convex bodies. The behavior of this algorithm w.r.t. its parameters is studied through numerical experiments, which also highlight the by-design robustness of the depth-trimmed regions based distance.

2 Background on Data-Depth

In this section, we recall the concept of statistical *data depth* function and its attractive theoretical properties for clarity. Here and throughout, the space of all continuous probability measures on \mathbb{R}^d with $d \in \mathbb{N}^*$ is denoted by $\mathcal{M}_1(\mathbb{R}^d)$. By g_{\sharp} we denote the push-forward operator of the function g . Introduced by [26], the concept of data depth extends the notion of median to the multivariate setting. In other words, it measures the centrality of any element $x \in \mathbb{R}^d$ w.r.t. a probability distribution (respectively, a data set). Formally, a data depth is defined as follows:

$$\begin{aligned} D : \quad \mathbb{R}^d \times \mathcal{M}_1(\mathbb{R}^d) &\longrightarrow [0, 1], \\ (x, \rho) &\longmapsto D(x, \rho). \end{aligned} \quad (1)$$

We denote by $D(x, \rho)$ (or $D_{\rho}(x)$ for shortness) the depth of $x \in \mathbb{R}^d$ w.r.t. $\rho \in \mathcal{M}_1(\mathbb{R}^d)$. The higher $D(x, \rho)$, the deeper it is in ρ . The depth-induced median of ρ is then defined by the set attaining $\sup_{x \in \mathbb{R}^d} D(x, \rho)$. Since data depth naturally and in a nonparametric way defines a pre-order on \mathbb{R}^d w.r.t. a probability distribution, it can be seen as a centrality-based alternative to the cumulative distribution function (cdf) for multivariate data. For any $\alpha \in [0, 1]$, the associated α -depth region of a depth function is defined as its upper-level set:

$$D_{\rho}^{\alpha} = \{x \in \mathbb{R}^d, D_{\rho}(x) \geq \alpha\}. \quad (2)$$

It follows that depth regions are nested, *i.e.* $D_{\rho}^{\alpha'} \subseteq D_{\rho}^{\alpha}$ for any $\alpha < \alpha'$. These depth regions generalize the notion of quantiles to a multivariate distribution.

The relevance of a depth function to capture the information about a distribution relies on the statistical properties it satisfies. Such properties have been thoroughly investigated in [29, 34, 45] with slightly different sets of axioms (or postulates) to be satisfied by a proper depth function. In this paper, we restrict to *convex depth functions* [45] mainly motivated by recent algorithmic developments including theoretical results [46] as well as implementation guidelines [33].

Clearly, (1) opens the door to a variety of possible definitions. While these differ in theoretical and practically-related properties such as robustness or computational complexity (see [35] for a detailed discussion), several postulates have been developed throughout the recent decades the “good” depth function should satisfy. Formally, a function D is called a *convex depth function* if it satisfies the following postulates:

D1 (AFFINE INVARIANCE) $D(g(x), g_{\sharp}\rho) = D(x, \rho)$ holds for $g : x \in \mathbb{R}^d \mapsto Ax + b$ with any non singular matrix $A \in \mathbb{R}^{d \times d}$ and any vector $b \in \mathbb{R}^d$.

D2 (VANISHING AT INFINITY) $\lim_{\|x\| \rightarrow \infty} D_{\rho}(x) = 0$.

D3 (UPPER SEMICONTINUITY) $\{x \in \mathbb{R}^d \mid D_{\rho}(x) < \alpha\}$ is an open set for every $\alpha \in (0, 1]$.

D4 (QUASICONCAVITY) For every $\lambda \in [0, 1]$ and $x, y \in \mathbb{R}^d$, $D_{\rho}(\lambda x + (1 - \lambda)y) \geq \min\{D_{\rho}(x), D_{\rho}(y)\}$.

While (D1) is useful in applications providing independence w.r.t. the measurement units and coordinate system, (D2) and (D3) appear as natural properties since data depth is a generalization of cdf. Limit values vanish due to median-oriented construction. (D4) allows to preserve the original center-outward ordering goal of data depth and induces convexity of the depth regions. Furthermore, it is easy to see that (D1–D4) respectively yield properties of affine equivariance, boundedness, closedness and convexity of the central regions D_{ρ}^{α} [45]. Thanks to (D2–D4), If $\alpha > 0$, non-empty regions associated to convex depth functions are convex bodies, *i.e.* compact convex set in \mathbb{R}^d . Below we recall two convex depth functions that belong to the computationally advantageous family of depths that satisfy the (weak) projection property [47], and thus can be efficiently and precisely approximated: halfspace depth, which is probably the most studied in the literature, and projection depth. For this, let \mathbb{S}^{d-1} be the unit sphere in \mathbb{R}^d and X a random variable defined on a certain probability space $(\Omega, \mathcal{A}, \mathbb{P})$ that takes values in $\mathcal{X} \subset \mathbb{R}^d$ following distribution ρ . The halfspace

depth of a given $x \in \mathbb{R}^d$ w.r.t. ρ is defined as the smallest probability mass that can be contained in a closed halfspace containing x :

$$HD_\rho(x) = \inf_{u \in \mathbb{S}^{d-1}} \mathbb{P}(\langle u, X \rangle \leq \langle u, x \rangle). \quad (3)$$

Projection depth, being a monotone transform of the Stahel-Donoho outlyingness [48, 49], is defined as follows:

$$PD_\rho(x) = \frac{1}{1 + O_\rho(x)} \quad \text{with} \quad O_\rho(x) = \sup_{u \in \mathbb{S}^{d-1}} \frac{|\langle u, x \rangle - \text{med}(\langle u, X \rangle)|}{\text{MAD}(\langle u, X \rangle)}, \quad (4)$$

where med and MAD stand for the univariate median and median absolute deviation from the median, respectively.

3 A Pseudo-Metric based on Depth-Trimmed Regions

In this section, we introduce the depth-based pseudo-metric and study its properties. Let μ, ν be two continuous probability measures on $\mathcal{X}, \mathcal{Y} \subset \mathbb{R}^d$ respectively. By $d_{\mathcal{H}}(A, B)$ is meant the Hausdorff distance between the sets A and B . We denote by $\alpha_{\max}(\mu) = \sup\{D_\mu(x), x \in \mathbb{R}^d\}$ the depth attained by the depth-induced median, which is itself the maximum level of the non-empty set D_μ^α . As a first go, we introduce the pseudo-metric between probability distributions μ and ν based on the depth-trimmed regions.

Definition 1. Let $\varepsilon \geq 0$, and set $\alpha^* = \min\{\alpha_{\max}(\mu), \alpha_{\max}(\nu)\}$. For all pairs (μ, ν) in $\mathcal{M}_1(\mathcal{X}) \times \mathcal{M}_1(\mathcal{Y})$, let $D_\mu(z)$ and $D_\nu(z)$ be any convex data depths of z w.r.t. μ and ν , respectively. The depth-trimmed regions ($DR_{p,\varepsilon}$) discrepancy measure between μ and ν is defined as

$$DR_{p,\varepsilon}(\mu, \nu) = \left(\frac{1}{\alpha^* - \varepsilon} \int_\varepsilon^{\alpha^*} d_{\mathcal{H}}(D_\mu^\alpha, D_\nu^\alpha)^p d\alpha \right)^{1/p}. \quad (5)$$

Because of the classic convention adopted to define the Hausdorff distance, we have $d_{\mathcal{H}}(D_\mu^\alpha, D_\nu^\alpha)^p = \infty$ as soon as at least one of the two regions is empty, which is the case only when $\alpha > \alpha^*$. Furthermore, properties (D2–D3) ensure that for every $\alpha > 0$, D_μ^α is a compact subset of \mathbb{R}^d yielding a well-defined metric. Observe that the parameter ε can be considered as a robustness tuning parameter. Indeed, choosing a higher ε amounts to ignore the account of the larger upper-level sets of the data depth, *i.e.* the tails of the distributions.

Remark 1. When $d = 1$, the L_p -Wasserstein distance enjoys an explicit expression involving quantile and distribution functions. Let $X^1 \sim \mu_1$, $Y^1 \sim \nu_1$ be two random variables where μ_1, ν_1 are univariate probability distributions. Denoting by $F_{X^1}^{-1}$ the quantile function of X^1 , the L_p -Wasserstein distance can be written as

$$W_p(\mu_1, \nu_1) = \left(\int_0^1 |F_{X^1}^{-1}(q) - F_{Y^1}^{-1}(q)|^p dq \right)^{1/p}. \quad (6)$$

Since data depth and its central regions are extensions of cdf and quantiles to dimension $d > 1$, $DR_{p,\varepsilon}$ is then a possible generalization of eq. (6) to higher dimensions.

3.1 Metric Properties

We now investigate to which extent the proposed discrepancy measure satisfies the metric axioms. As a first go, we show that $DR_{p,\varepsilon}$ fulfills most conditions but does not define a distance in general and exhibit specific situations where it does.

Proposition 1 (METRIC PROPERTIES). For any (convex) data depth, $DR_{p,\varepsilon}$ is positive, symmetric and satisfies triangular inequality but the entailment $DR_{p,\varepsilon}(\mu, \nu) = 0 \implies \mu = \nu$ does not hold in general. In addition, $DR_{p,\varepsilon}$ is a distance if and only if the upper level sets of the chosen data depth fully characterize probability distributions.

Thus, $DR_{p,\varepsilon}$ (while not always fulfilling the separation condition) defines a pseudo-metric rather than a distance. However, certain data depths introduced in the literature actually characterize probability

distributions under mild assumptions. For example, it is the case of the zonoid depth for random variables with finite first moments [50] or of the halfspace depth under further assumptions on the distribution [51, 52, 53]. Although this is not the case for the halfspace depth in full generality, as highlighted in [54], such a data depth characterizes all empirical distributions [55]. Hence, in practice, the pseudo-metric we introduced nearly behaves as a distance. In the remainder of the paper, we do not distinguish the cases where it defines a distance or not and might call it abusively 'distance' for simplicity. The next proposition describes the behavior of the proposed discrepancy measure under specific transformations.

Proposition 2 (ISOMETRY INVARIANCE). *Let $A \in \mathbb{R}^{d \times d}$ be a non singular matrix and $b \in \mathbb{R}^d$. Define the isometry mapping $g : x \in \mathbb{R}^d \mapsto Ax + b$ with $AA^\top = I_d$, then it holds:*

$$DR_{p,\varepsilon}(g_\sharp\mu, g_\sharp\nu) = DR_{p,\varepsilon}(\mu, \nu).$$

In particular, it ensures invariance of $DR_{p,\varepsilon}$ under translations and rotations.

Although formulas (5) and (6) are based on the same spirit, there are not apparent reasons why the proposed pseudo-metric should have the same behavior as the Wasserstein distance. Proposition 3 investigates the ability to factor out translations, for $DR_{2,\varepsilon}$ associated with the halfspace depth, giving a positive answer for the case of two Gaussian distributions with equal covariance matrices.

Proposition 3 (TRANSLATION CHARACTERIZATION). *Consider X, Y two random variables from $\mu \in \mathcal{M}_1(\mathcal{X})$ and $\nu \in \mathcal{M}_1(\mathcal{Y})$ with expectations $\mathbf{m}_1, \mathbf{m}_2$ and variance-covariance matrices Σ_1, Σ_2 respectively. Denoting by μ^*, ν^* their centered version, it holds:*

$$\left| DR_{2,\varepsilon}^2(\mu, \nu) - DR_{2,\varepsilon}^2(\mu^*, \nu^*) - \|\mathbf{m}_1 - \mathbf{m}_2\|^2 \right| \leq 2 DR_{1,\varepsilon}(\mu^*, \nu^*) \|\mathbf{m}_1 - \mathbf{m}_2\|.$$

Now, let $\mu \sim \mathcal{N}(\mathbf{m}_1, \Sigma_1)$ and $\nu \sim \mathcal{N}(\mathbf{m}_2, \Sigma_2)$. Then it holds:

$$\left| DR_{1,\varepsilon}(\mu, \nu) - \|\mathbf{m}_1 - \mathbf{m}_2\| \right| \leq C_\varepsilon \sup_{u \in \mathbb{S}^{d-1}} \left| \sqrt{u^\top \Sigma_1 u} - \sqrt{u^\top \Sigma_2 u} \right|,$$

where $C_\varepsilon = \int_\varepsilon^{\alpha^} |\Phi^{-1}(1 - \alpha)| d\alpha$ with Φ the cdf of the univariate standard Gaussian distribution.*

This proposition shows that $DR_{2,\varepsilon}$ is able to factor out translations in a similar way as Wasserstein distance if $DR_{1,\varepsilon}(\mu^*, \nu^*)$ is zero. Assuming that conditions of Proposition 1 are satisfied, it holds only if $\mu^* \neq \nu^*$. Furthermore, it is clear that if $DR_{1,\varepsilon}(\mu^*, \nu^*) = 0$ then $DR_{2,\varepsilon}(\mu^*, \nu^*)$ is zero too. It leads to an interesting consequence of Proposition 3: when $\Sigma_1 = \Sigma_2$, one has $DR_{2,\varepsilon}(\mu, \nu) = DR_{1,\varepsilon}(\mu, \nu) = \|\mathbf{m}_1 - \mathbf{m}_2\|$ for any $\mu \sim \mathcal{N}(\mathbf{m}_1, \Sigma_1)$ and $\nu \sim \mathcal{N}(\mathbf{m}_2, \Sigma_2)$.

3.2 Sample Versions - Statistical Properties

We now study asymptotic, as well as non-asymptotic, statistical properties of the empirical version of $DR_{p,\varepsilon}$. Given a sample X_1, \dots, X_n composed of i.i.d. observations drawn from distribution μ , consider the empirical measure $\hat{\mu}_n = (1/n) \sum_{i=1}^n \delta_{X_i}$, where δ_x denotes the Dirac mass at any point x . Precisely, the questions we seek to answer here can be formulated as follows: does $DR_{p,\varepsilon}(\hat{\mu}_n, \mu)$ converge to zero ? And if so, how fast is the convergence?

As a first go, we derive sufficient conditions under which almost sure convergence is satisfied by $DR_{p,\varepsilon}(\hat{\mu}_n, \mu)$. They essentially result from the data depth convergence properties.

Proposition 4 (STRONG CONSISTENCY). *If $D_{\hat{\mu}_n}$ is uniformly convergent to D_μ , i.e. $\sup_{x \in \mathbb{R}^d} |D_{\hat{\mu}_n}(x) - D_\mu(x)| \xrightarrow{a.s.} 0$ when $n \rightarrow \infty$, and the mapping $\alpha \in [\varepsilon, \alpha_{\max}(\mu)] \mapsto D_\mu^\alpha$ is continuous w.r.t. the Hausdorff distance, then $DR_{p,\varepsilon}(\hat{\mu}_n, \mu) \xrightarrow{a.s.} 0$ when n tends to infinity.*

Most data depths are uniformly convergent, e.g. halfspace, projection and zonoid depths. Assessing convergence rates is much more difficult in general. To the best of our knowledge, until now convergence rates were only tackled in the case of halfspace depth in [56, 57]. In [58] pointwise (w.r.t. α) convergence rates, of order $O(1/\sqrt{n})$, of the halfspace regions are provided. In order to

establish non-asymptotic guarantees, additional assumptions are required. Avoiding the degenerate case where $D_\mu^{\alpha^*}$ is a singleton (*i.e.* a single point), there exist $a_\alpha, r_\alpha, R_\alpha$ such that $B(a_\alpha, r_\alpha) \subset D_\mu^\alpha \subset B(a_\alpha, R_\alpha)$ for any $\alpha \in [\varepsilon, \alpha^* - \varepsilon]$. Considering this, we restrict our analysis to $DR_{p,\varepsilon}^-$, defined by taking the integral over $\mathcal{I}_\varepsilon := [\varepsilon, \alpha^* - \varepsilon]$ instead of $[\varepsilon, \alpha^*]$.

Assumption 1. *Let $\gamma > 0$, then, for any $u \in \mathbb{S}^{d-1}$ and q', q in $[q_u^\varepsilon - \gamma, q_u^{\alpha^* - \varepsilon} + \gamma]$ or in $[q_u^{\alpha^* + \varepsilon} - \gamma, q_u^{1-\varepsilon} + \gamma]$, we have: $|F_u(q) - F_u(q')| \geq L|q - q'|$.*

Assumption 2. *We have: $\inf_{\alpha \in \mathcal{I}_\varepsilon} r_\alpha > \gamma$.*

Assumption 1 can be seen as an extension of Assumption 1 in [58] to the uniform setting. The following result provides a tail bound for $DR_p^-(\hat{\mu}_n, \mu)$ of order $O_{\mathbb{P}}(1/\sqrt{n})$ meeting the expectations. It does not suffer from the curse of the dimensionality, growing sublinearly with d .

Theorem 1 (CONVERGENCE RATE). *For the halfspace depth function, suppose that Assumptions 1-2 are satisfied. Then, for any $\delta \in (e^{-250(d+1)(1+L)/L}, 1)$, it holds with probability at least $1 - \delta$:*

$$DR_{p,\varepsilon}^-(\mu_n, \mu) \leq \kappa_1 \sqrt{\frac{d+1}{n}} + \kappa_2 \sqrt{\frac{\log(1/\delta)}{n}},$$

with $\kappa_1 = (10\sqrt{5} \sup_{\alpha \in \mathcal{I}_\varepsilon} c_\alpha)/L + \sup_{\alpha \in \mathcal{I}_\varepsilon} c_\alpha (10\sqrt{5} - 1)/\sqrt{L}$, $\kappa_2 = \sup_{\alpha \in \mathcal{I}_\varepsilon} c_\alpha \sqrt{2/L}$, and $c_\alpha = \frac{R_\alpha}{r_\alpha} \frac{1+\gamma/r_\alpha}{1-\gamma/r_\alpha}$.

3.3 Robustness

In this part, we explore the robustness of the proposed distance, associated with the halfspace depth, in view of the finite sample breakdown point (BP) [59, 60]. This notion investigates the smallest contamination fraction under which the estimation breaks down in the worst case. Considering a sample $\mathcal{S}_n = \{X_1, \dots, X_n\}$ composed of i.i.d. observations drawn from a distribution μ with empirical measure $\hat{\mu}_n = (1/n) \sum_{i=1}^n \delta_{X_i}$, the finite sample breakdown point of $DR_{p,\varepsilon}$ w.r.t. \mathcal{S}_n is defined as

$$BP(DR_{p,\varepsilon}, \mathcal{S}_n) = \min \left\{ \frac{o}{n+o} : \sup_{Z_1, \dots, Z_o} DR_{p,\varepsilon}(\hat{\mu}_{n+o}, \hat{\mu}_n) = +\infty \right\},$$

where $\hat{\mu}_{n+o} = \frac{1}{n+o} \left(\sum_{i=1}^n \delta_{X_i} + \sum_{j=1}^o \delta_{Z_j} \right)$ is the "concatenate" empirical measure between X_1, \dots, X_n and the contamination sample Z_1, \dots, Z_o with $o \in \mathbb{N}^*$. It is well known that the extremal regions of the halfspace depth are not robust while its central regions are rather stable under contamination [48]. Fortunately, by construction, the parameter ε allows to ignore these extremal depth regions and thus to ensure robustness of the depth-trimmed regions distance. Based on results of [48, 61], the following proposition provides a lower bound on the finite sample breakdown point of $DR_{p,\varepsilon}$ which highlights the robustness of the proposed distance (as well as its dependence on ε).

Proposition 5 (BREAKDOWN POINT). *For the halfspace depth function, let $\alpha_{\max}(\hat{\mu}_n)$ be the maximal depth w.r.t. \mathcal{S}_n . Then for any $\varepsilon < \alpha_{\max}(\hat{\mu}_n)$, it holds*

$$BP(DR_{p,\varepsilon}, \mathcal{S}_n) \geq \begin{cases} \frac{\lceil n\varepsilon/(1-\varepsilon) \rceil}{n + \lceil n\varepsilon/(1-\varepsilon) \rceil} & \text{if } \varepsilon \leq \frac{\alpha_{\max}(\hat{\mu}_n)}{1 + \alpha_{\max}(\hat{\mu}_n)}, \\ \frac{\alpha_{\max}(\hat{\mu}_n)}{1 + \alpha_{\max}(\hat{\mu}_n)} & \text{otherwise.} \end{cases}$$

Thus, at least a proportion $\varepsilon/(1-\varepsilon)$ of outliers must be added to break down $DR_{p,\varepsilon}$ when considering larger regions, while central regions are robust independently of ε . Between two data sets, $DR_{p,\varepsilon}$ breaks down if depth regions for at least one of the data sets do. The breakdown point is then the minimum between the BP of each data set. However, the breakdown point considers the worst case, *i.e.* the supremum over all possible contaminations, and is often pessimistic. Indeed the proposed pseudo-metric can handle more outliers in several cases as experimentally illustrated in Section 5.

4 Efficient Approximate Computation

Exact computation of $DR_{p,\varepsilon}$ can appear time-consuming, due to the high time complexity of the algorithms that calculate depth-trimmed regions (c.f. [62, 63] for projection and halfspace depths, respectively) rapidly growing with dimension. However, we design a universal approximate algorithm that achieves (log-) linear time complexity in n . Since properties D2-D3-D4 ensure that depth regions are convex bodies in \mathbb{R}^d , they can be characterized by support functions, *i.e.* for a convex compact \mathcal{K} , $h_{\mathcal{K}}(u) = \sup\{\langle x, u \rangle, x \in \mathcal{K}\}$. Following [64], for two (convex) regions D_{μ}^{α} and D_{ν}^{α} , the Hausdorff distance between them can be calculated as:

$$d_{\mathcal{H}}(D_{\mu}^{\alpha}, D_{\nu}^{\alpha}) = \sup_{u \in \mathbb{S}^{d-1}} |h_{D_{\mu}^{\alpha}}(u) - h_{D_{\nu}^{\alpha}}(u)|.$$

As we shall see in Section 5, mutual approximation of $h_{D_{\mu}^{\alpha}}(u)$ by points from the sample and of $h_{D_{\nu}^{\alpha}}(u)$ by taking maximum over a finite set of directions allows for stable estimation quality. Recently, motivated by their numerous applications, a plethora of algorithms have been developed for (exact and approximate) computation of data depths. Depths satisfying the projection property (which also include halfspace and projection depth, see [45]) can be approximated by taking minimum over univariate depths; see *e.g.* [65, 66, 62], [46] for theoretical guarantees, and [33] for an experimental validation. Let \mathbf{X}, \mathbf{Y} be two samples $\mathbf{X} = \{X_1, \dots, X_n\}$ and $\mathbf{Y} = \{Y_1, \dots, Y_m\}$ from μ, ν . When calculating approximated depth of sample points $D^{\mathbf{X}} = \{D(X_i, \hat{\mu}_n)\}_{i=1}^n$ (respectively $D^{\mathbf{Y}}$), a matrix $\mathbf{M}^{\mathbf{X}}$ (respectively $\mathbf{M}^{\mathbf{Y}}$) of projections of sample points on (a common) set of K directions (with its element $\mathbf{M}_{i,k}^{\mathbf{X}} = \langle u_k, X_i \rangle$ for some $u_k \sim \mathcal{U}(\mathbb{S}^{d-1})$) can be obtained as a side product. More precisely, $D^{\mathbf{X}}, D^{\mathbf{Y}}, \mathbf{M}^{\mathbf{X}}, \mathbf{M}^{\mathbf{Y}}$ are used in Algorithm 1, which implements the MC-approximation of the integral in (5). Particular cases of approximation algorithms for the halfspace depth and the projection depth are recalled in Section C in the Supplementary Material.

Algorithm 1 Approximation of $DR_{p,\varepsilon}$

Initialization: n_{α}, K .

```

1:  $H = 0$ ; compute  $D^{\mathbf{X}}, D^{\mathbf{Y}}, \mathbf{M}^{\mathbf{X}}, \mathbf{M}^{\mathbf{Y}}$ .
2: Draw  $\alpha_{\ell} \sim \mathcal{U}([\varepsilon, \hat{\alpha}^*]), \ell = 1, \dots, n_{\alpha}$  with  $\hat{\alpha}^* = \min\{\max D^{\mathbf{X}}, \max D^{\mathbf{Y}}\}$ .
3: for  $\ell = 1, \dots, n_{\alpha}$  do
4:   Determine points inside  $\alpha_{\ell}$ -region:  $\mathcal{I}_{\alpha_{\ell}}^{\mathbf{X}} = \{i : D_i^{\mathbf{X}} > \alpha_{\ell}\}; \mathcal{I}_{\alpha_{\ell}}^{\mathbf{Y}} = \{j : D_j^{\mathbf{Y}} > \alpha_{\ell}\}$ .
5:   for  $k = 1, \dots, K$  do
6:     Compute approximation of support functions:  $h_k^{\mathbf{X}} = \max \mathbf{M}_{\mathcal{I}_{\alpha_{\ell}}^{\mathbf{X}}, k}^{\mathbf{X}}; h_k^{\mathbf{Y}} = \max \mathbf{M}_{\mathcal{I}_{\alpha_{\ell}}^{\mathbf{Y}}, k}^{\mathbf{Y}}$ .
7:   end for
8:   Increase cumulative Hausdorff distance:  $H += \max_{k \leq K} |h_k^{\mathbf{X}} - h_k^{\mathbf{Y}}|^p$ .
9: end for
Output:  $\widehat{DR}_{p,\varepsilon} = (H/n_{\alpha})^{1/p}$ .
```

Time complexity of Algorithm 1 is $O(K(\Omega.(n \vee m, d) \vee n_{\alpha}(n \vee m)))$, where $\Omega(\cdot, \cdot)$ stands for the complete complexity of computing univariate depths—in projections on u —for all points of the sample. As a byproduct, projections on u can be saved to be reused after for the approximation of $h_{D_{\mu}^{\alpha}}(u)$. *E.g.*, for the halfspace depth $\Omega_{hsp}(n, d) = O(n(d \vee \log n))$ composed of projection of the data onto u , ordering them, and passing to record the depths (see *e.g.* [67]). For the projection depth $\Omega_{prj}(n, d) = O(nd)$, where after projecting the data onto u , univariate median and MAD can be computed with complexity $O(n)$ (see *e.g.* [62]).

5 Numerical Experiments

In this section, we first explore the quality of the approximation introduced in Section 4 depending on the number of projections. Further, robustness of the proposed pseudo-metric $DR_{p,\varepsilon}$ to outliers is investigated in three different settings. Finally, the good behavior of $DR_{p,\varepsilon}$ is demonstrated when applied to clustering. Where applicable, we include state-of-the-art methods for comparison. Due to space limitations, experiments on the influence of the parameter n_{α} as well as several toy examples on real large-scale data sets (Fashion-MNIST and Movies) are deferred to the Supplementary Material.

The choice of the number of projections. Proposition 3 allows to derive a closed form expression for $DR_{2,\varepsilon}(\mu, \nu)$ when μ, ν are Gaussian distributions with the same variance-covariance matrix. In

order to investigate the quality of the approximation on light-tailed and heavy-tailed distributions, we focus on computing $DR_{2,0}$ (with $n_\alpha = 20$) for varying number of random projections K between a sample of 1000 points stemming from $\mu \sim \mathcal{N}(\mathbf{0}_d, I_d)$ for $d \in \{5, 50\}$ and three different samples (which yields six settings). These three samples are constructed from 1000 observations stemming from *Gaussian*, *Student-t₂* and *Cauchy* distributions all with an expectation equal to $\mathbf{7}_d$. Comparison with the approximation of max Sliced-Wasserstein (max-SW) (see *e.g.* [23]), which shares the same closed-form as $DR_{2,0}$, is also provided. Denoting by $\widehat{\text{max-SW}}$ the Monte-Carlo approximation of the max-SW, the relative approximation errors, *i.e.*, $(\widehat{DR}_{p,0} - \|\mathbf{7}_d\|_2)/\|\mathbf{7}_d\|_2$ and $(\text{max-SW} - \|\mathbf{7}_d\|_2)/\|\mathbf{7}_d\|_2$, are computed investigating both the quality of the approximation and the robustness of these distances. Results, that report the averaged approximation error as well as the 25-75% empirical quantile intervals are depicted in Figure 4. They show that $DR_{p,0}$ possesses the same behavior as max-SW when considering *Gaussians* and *Student-t₂*, while it behaves advantageously for *Cauchy* distribution. The approximation error converges to zero with growing K with faster speed when d is smaller.

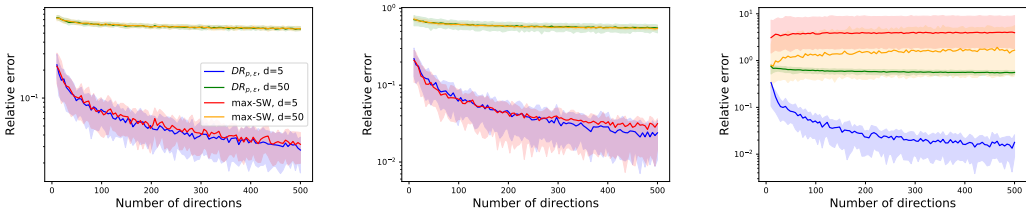


Figure 1: Relative approximation error (averaged over 100 repetitions) of $DR_{p,\varepsilon}$ and the max Sliced-Wasserstein for *Gaussian* (left), *Student-t₂* (middle) and *Cauchy* (right) distributions for differing numbers of approximating directions.

Robustness to outliers. We analyze the robustness of $DR_{p,\varepsilon}$ by measuring its ability to overcome outliers. In this benchmark we naturally include existing robust extensions of the Wasserstein distance: Subspace Robust Wasserstein (*SRW*) [68] searching for a maximal distance on lower-dimensional subspaces, *ROBOT* [69] and *RobustOT* [70] being robust modifications of the unbalanced optimal transport [71]. Medians-of-Means Wasserstein (*MoMW*) [72], that replaces the empirical means in the Kantorovich duality formulae by the robust mean estimator MoM (see, *e.g.*, [73, 74]), is not employed due to high computational burden. Further, for completeness, we add the standard Wasserstein distance (*W*) and its approximation the Sliced-Wasserstein (*SW*) distance with the same number of projections ($K = 1000$) as $DR_{p,\varepsilon}$. Since the scales of the compared methods differ, *relative error* is used as a performance metric, *i.e.*, the ratio of the absolute difference of the computed distance with and without anomalies divided by the latter. Three settings for a pair of distributions are addressed: (a) *Fragmented hypercube* precedently studied in [68, 75], where the source distribution is uniform in the hypercube $[-1, 1]^2$ and the target distribution is transformed from the source via the map $T : x \mapsto x + 2\text{sign}(x)$ where $\text{sign}(\cdot)$ is taken element-wisely. Outliers are drawn uniformly from $[-4, 4]^2$. (b) *Circles* data set from *scikit-learn* [76] Python library with noise parameter 0.2 and outliers drawn uniformly in the unit ball in \mathbb{R}^2 . (c) Two multivariate standard *Gaussian* distributions, one shifted by 10_2 , with outliers drawn uniformly from $[-10, 20]^2$. Our analysis is conducted over 500 sampled points from the distributions described above. In order to have meaningful values of ε , we consider the empirical quantiles τ_1, τ_2, τ_3 of the data depth computed on source and target distributions such that 10%, 20%, 30% of data with lower depth values w.r.t. each distribution are not used in computation of $DR_{p,\tau_1}, DR_{p,\tau_2}, DR_{p,\tau_3}$, respectively. Figure 2, which plots the relative error (averaged over 100 random repetitions) depending on the portion of outliers varying up to 20%, illustrates advantageous behavior of $DR_{p,\varepsilon}$ (for $\varepsilon = \tau_1, \tau_2, \tau_3$) for reasonable (starting with $\approx 2.5\%$) contamination.

Clustering. We demonstrate the relevance of the proposed pseudo-metric through an application to (robust) clustering. To that end, we perform spectral clustering [77] on two data sets derived from Fashion-MNIST. Each gray scale image is seen as a bag of pixels [78], *i.e.* as an empirical probability distribution over a 3-dimensional space (the two first dimensions indicate the pixel position and the third one, its intensity). The first data set is constructed taking the 100 first images in each class of the Fashion-MNIST data set. The second data set, considered as contaminated, is designed

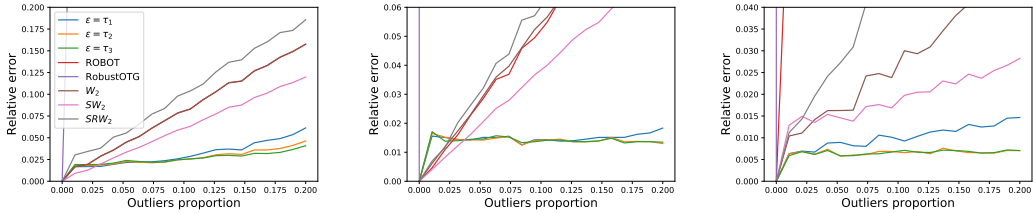


Figure 2: Relative error (averaged over 100 repetitions) of different distances for increasing portion of outliers for *fragmented hypercube* (left), *circles* (middle) and *Gaussian* data sets (right).

by introducing white patches on the left corner of 50 images drawn uniformly in the first data set, which yields 5% of contamination. We benchmark $DR_{p,\varepsilon}$ setting $p = 2$ and $\varepsilon = 0$ with the Wasserstein, the Sliced-Wasserstein and the Maximum Mean Discrepancy (MMD) [79] distances. $DR_{p,\varepsilon}$ and the Sliced-Wasserstein are approximated by Monte-Carlo using 100 directions while the MMD distance is computed using a Gaussian kernel with bandwidth equal to 1. As a baseline method, spectral clustering is also applied on images considered as vectors using euclidian distance. Standard parameters of the `scikit-learn` [76] spectral clustering implementation are employed with a number of clusters fixed to 10. Performance of the benchmarked metrics are assessed by measuring the normalized mutual information (NMI) [80] and the adjusted rank index (ARI) [81], which are standard clustering evaluation measures when the ground truth class labels are available. Results presented in Table 1 show the outperformance of $DR_{p,\varepsilon}$ over classical metrics.

		$DR_{p,\varepsilon}$	Wasserstein	Sliced-Wasserstein	MMD	Euclidian
Fashion-MNIST	NMI	0.58	0.50	0.55	0.54	0.50
	ARI	0.43	0.35	0.39	0.37	0.32
Corrupted Fashion-MNIST	NMI	0.55	0.48	0.47	0.50	0.48
	ARI	0.42	0.30	0.33	0.36	0.30

Table 1: Spectral clustering performances calculated using different metrics.

6 Concluding Remarks

Leveraging the notion of statistical data depth function, a novel pseudo-metric between multivariate probability distributions—that meets the aforementioned requirements—was introduced (see the overview in Table 2). This discrepancy measure inherits geometrical properties from data depth through affine transformation as well as parametric convergence rate growing sublinearly with the dimension. Overall, this framework exhibits an inherent versatility due to the existence of numerous data depths variants. The linear approximation algorithm and the robustness property make $DR_{p,\varepsilon}$ a promising tool for a large spectrum of applications beyond clustering, *e.g.* in generative adversarial networks (GANs) or in information retrieval.

	Pseudo-metric	Isometry Invariance	TC	Consistency	Bound	Fast approximation
Halfspace	✓	✓	✓	✓	✓	✓
Projection	✓	✓	✗	✓	✗	✓

Table 2: Properties satisfied by $DR_{p,\varepsilon}$ associated with the halfspace and projection depths. TC stands for the Translation Characterization property.

Moreover, recent works, extending the notion of data depth to further types of data such as functional and time-series data [82, 42], directional (or spherical) data [83], random matrices [84], curves (or paths) data [85], random sets [86], and graphs [87], shall allow for the use of the proposed pseudo-metric for a wide range of applications.

Acknowledgments

This work has been funded by BPI France in the context of the PSPC Project Expresso (2017-2021).

References

- [1] Solomon Kullback. *Information Theory and Statistics*. John Wiley, 1959.
- [2] Alfréd Rényi. On measures of entropy and information. In *Proceedings of the 4th Berkeley Symposium on Mathematical Statistics and Probability, Volume 1: Contributions to the Theory of Statistics*, pages 547–561, Berkeley, Calif., 1961. University of California Press.
- [3] Imre Csiszár. Eine informationstheoretische ungleichung und ihre anwendung auf den bewis der ergodizität von markhoffschen kette. *Magyar Tud. Akad. Mat. Kutato Int. Kozl.*, 8:85–108, 1963.
- [4] Wolfgang Stummer and Igor Vajda. On bregman distances and divergences of probability measures. *IEEE Transactions on Information Theory*, 58(3):1277 – 1288, 2012.
- [5] Patrick Billingsley. *Convergence of probability measures (2nd ed.)*. John Wiley & Sons, 1999.
- [6] Bharath K. Sriperumbudur, Kenji Fukumizu, Arthur Gretton, Bernhard Schölkopf, and Gert R. G. Lanckriet. On the empirical estimation of integral probability metrics. *Electron. J. Statist.*, 6:1550–1599, 2012.
- [7] Victor M. Panaretos and Yoav Zemel. Statistical aspects of wasserstein distances. *Annual Review of Statistics and Its Application*, 6(1):405–431, 2019.
- [8] S.T. Rachev. *Probability Metrics and the Stability of Stochastic Models*. Wiley Series in Probability and Statistics - Applied Probability and Statistics Section. Wiley, 1991.
- [9] Sung-Hyuk Cha and Sargur N. Srihari. On measuring the distance between histograms. *Pattern Recognit.*, 35(6):1355–1370, 2002.
- [10] David JC MacKay and David JC Mac Kay. *Information theory, inference and learning algorithms*. Cambridge university press, 2003.
- [11] Michael Irwin Jordan. *Learning in graphical models*, volume 89. Springer Science & Business Media, 1998.
- [12] Ian Goodfellow, Jean Pouget-Abadie, Mehdi Mirza, Bing Xu, David Warde-Farley, Sherjil Ozair, Aaron Courville, and Yoshua Bengio. Generative adversarial networks. *Communications of the ACM*, 63(11):139–144, 2020.
- [13] David M Blei, Alp Kucukelbir, and Jon D McAuliffe. Variational inference: A review for statisticians. *Journal of the American statistical Association*, 112(518):859–877, 2017.
- [14] Cedric Villani. *Topics in Optimal Transportation*. Graduate Studies in Mathematics Series. American Mathematical Society, New York, 2003.
- [15] Filippo Santambrogio. *Optimal Transport for Applied Mathematicians*. Birkhauser, 2015.
- [16] Gabriel Peyré and Marco Cuturi. Computational optimal transport. *Foundations and Trends® in Machine Learning*, 11(5-6):355–607, 2019.
- [17] Martin Arjovsky, Soumith Chintala, and Léon Bottou. Wasserstein gan, 2017. arXiv preprint arXiv:1701.07875.
- [18] Nicolas Courty, Rémi Flamary, and Devis Tuia. Domain adaptation with regularized optimal transport. In Toon Calders, Floriana Esposito, Eyke Hüllermeier, and Rosa Meo, editors, *Machine Learning and Knowledge Discovery in Databases*, pages 274–289, 2014.
- [19] Robert. M. Dudley. The speed of mean glivenko-cantelli convergence. *Ann. Math. Statist.*, 40(1):40–50, 02 1969.
- [20] Marco Cuturi, Olivier Teboul, and Jean-Philippe Vert. Sinkhorn distances: Lightspeed computation of optimal transportation. In *Advances in Neural Information Processing Systems (NeurIPS 2013)*, 2013.
- [21] Aude Genevay, Marco Cuturi, Gabriel Peyré, and Francis Bach. Stochastic Optimization for Large-scale Optimal Transport. In *NIPS 2016 - Thirtieth Annual Conference on Neural Information Processing System*, 2016.

- [22] Nicolas Bonneel, Julien Rabin, Gabriel Peyré, and Hanspeter Pfister. Sliced and radon wasserstein barycenters of measures. *Journal of Mathematical Imaging and Vision*, 51:22–45, 2015.
- [23] Soheil Kolouri, Kimia Nadjahi, Simsekli Umut, Roland Badeau, and Gustavo Rohde K. Generalized sliced wasserstein distance. In *Proceedings of the 33rd Conference on Neural Information Processing Systems (NeurIPS)*, 2019.
- [24] John H.J. Einmahl and David M. Mason. Generalized quantile process. *The annals of statistics*, 1992.
- [25] Vladimir I. Koltchinskii and Robert M. Dudley. On spatial quantiles. *Unpublished manuscript*, 1996.
- [26] John W. Tukey. Mathematics and the picturing of data. In R.D. James, editor, *Proceedings of the International Congress of Mathematicians*, volume 2, pages 523–531. Canadian Mathematical Congress, 1975.
- [27] Karl Mosler. Depth statistics. *Robustness and complex data structures*, 2013.
- [28] Vic Barnett. The ordering of multivariate data. *Journal of the royal society A*, 1976.
- [29] Regina Y. Liu. On a notion of data depth based on random simplices. *The Annals of Statistics*, 18(1):405–414, 1990.
- [30] Hannu Oja. Descriptive statistics for multivariate distributions. *Statistics and Probability Letters*, 1983.
- [31] Gleb Koshevoy and Karl Mosler. Zonoid trimming for multivariate distributions. *The Annals of Statistics*, 25(5):1998–2017, 10 1997.
- [32] Oleksii Pokotylo, Pavlo Mozharovskyi, and Rainer Dyckerhoff. Depth and depth-based classification with R-Package ddalpha. *Journal of Statistical Software, Articles*, 91(5):1–46, 2019.
- [33] Rainer Dyckerhoff, Pavlo Mozharovskyi, and Stanislav Nagy. Approximate computation of projection depths. *Computational Statistics and Data Analysis*, 2020. in press.
- [34] B.Y. Zuo and R. Serfling. General notions of statistical depth function. *The Annals of Statistics*, 28(2):461–482, 2000.
- [35] Karl Mosler and Pavlo Mozharovskyi. Choosing among notions of depth for multivariate data. *Statistical Science*, 2021. in press.
- [36] Peter J. Rousseeuw and Mia Hubert. Regression depth. *Journal of the American Statistical Association*, 94(446):388–402, 1999.
- [37] Marc Hallin, Davy Paindaveine, and Miroslav Šiman. Multivariate quantiles and multiple-output regression quantiles: From l_1 optimization to halfspace depth. *Ann. Statist.*, 38(2):635–669, 04 2010.
- [38] Jun Li, Juan A. Cuesta-Albertos, and Regina Y. Liu. Dd-classifier: Nonparametric classification procedure based on dd-plot. *JASA*, 107(498):737–753, 2012.
- [39] Tatjana Lange, Karl Mosler, and Pavlo Mozharovskyi. Fast nonparametric classification based on data depth. *Statistical Papers*, 55(1):49–69, 2014.
- [40] Robert Serfling. Depth functions in nonparametric multivariate inference. *DIMACS Series in Discrete Mathematics and Theoretical Computer Science*, 72, 2006.
- [41] Peter J. Rousseeuw and Mia Hubert. Anomaly detection by robust statistics. *WIREs Data Mining and Knowledge Discovery*, 8(2):1236, 2018.
- [42] Guillaume Staerman, Pavlo Mozharovskyi, and Stéphan Clémençon. The area of the convex hull of sampled curves: a robust functional statistical depth measure. In *Proceedings of the 23rd International Conference on Artificial Intelligence and Statistics (AISTATS 2020)*, volume 108, pages 570–579, 2020.
- [43] Guillaume Staerman, Pavlo Mozharovskyi, and Stéphan Clémençon. Affine-invariant integrated rank-weighted depth: Definition, properties and finite sample analysis, 2021. arXiv 2106.11068.
- [44] Rebecka Jörnsten. Clustering and classification based on the l_1 data depth. *Journal of Multivariate Analysis*, 90(1):67 – 89, 2004.
- [45] Rainer Dyckerhoff. Data depth satisfying the projection property. *Allgemeines Statistisches Archiv*, 88(2):163–190, 2004.

[46] Stanislav Nagy, Rainer Dyckerhoff, and Pavlo Mozharovskyi. Uniform convergence rates for the approximated halfspace and projection depth. *Electronic Journal of Statistics*, 14(2):3939–3975, 2020.

[47] Rainer Dyckerhoff. Data depths satisfying the projection property. *Allgemeines Statistisches Archiv*, 88(2):163–190, 2004.

[48] David L. Donoho and Miriam Gasko. Breakdown properties of location estimates based on half space depth and projected outlyingness. *The Annals of Statistics*, 20:1803–1827, 1992.

[49] Werner. A. Stahel. Breakdown of covariance estimators. Technical report, Fachgruppe für Statistik, ETH, Zürich, 1981.

[50] Karl Mosler. *Multivariate Dispersion, Central Regions, and Depth*. Springer, 2002.

[51] Abdelhamid Hassairi and Ons Regaieg. On the tukey depth of a continuous probability distribution. *Statistics & Probability Letters*, 78(15):2308 – 2313, 2008.

[52] Linglong Kong and Yijun Zuo. Smooth depth contours characterize the underlying distribution. *Journal of Multivariate Analysis*, 101(9):2222 – 2226, 2010.

[53] Stanislav Nagy, Carsten Schütt, and Elisabeth M. Werner. Halfspace depth and floating body. *Statist. Surv.*, 13:52–118, 2019.

[54] Stanislav Nagy. Halfspace depth does not characterize probability distributions. *Statistical Papers*, 2019.

[55] Anja J. Struyf and Peter J. Rousseeuw. Halfspace depth and regression depth characterize the empirical distribution. *Journal of Multivariate Analysis*, 69(1):135 – 153, 1999.

[56] Galen R. Shorack and John A. Wellner. Empirical processes with applications to statistics. Wiley, NY, 1986.

[57] Michael A. Burr and Robert J. Fabrizio. Uniform convergence rates for halfspace depth. *Statistics & Probability Letters*, 124:33 – 40, 2017.

[58] Victor-Emmanuel Brunel. Concentration of the empirical level sets of tukey’s halfspace depth. *Probability Theory and Related Fields*, 173(3):1165–1196, 2019.

[59] David L. Donoho. Breakdown properties of location estimators. *P.h.D., qualifying paper; Dept. Statistics, Harvard University*, 1982.

[60] David L. Donoho and Peter J. Hubert. The notion of breakdown point. *A Festschrift for Erich Lehman*, pages 157–184, 1983.

[61] Stanislav Nagy and Jiří Dvořák. Illumination depth. *Journal of Computational and Graphical Statistics*, 30(1):78–90, 2021.

[62] Xiaohui Liu and Yijun Zuo. Computing projection depth and its associated estimators. *Statistics and Computing*, 24(1):51–63, 2014.

[63] Xiaohui Liu, Karl Mosler, and Pavlo Mozharovskyi. Fast computation of tukey trimmed regions and median in dimension $p > 2$. *Journal of Computational and Graphical Statistics*, 28(3):682–697, 2019.

[64] Rolf Schneider. *Convex Bodies: The Brunn-Minkowski Theory*. Cambridge University Press, Cambridge, 1993.

[65] Peter J. Rousseeuw and Anja Struyf. Computing location depth and regression depth in higher dimensions. *Statistics and Computing*, 8(3):193–203, 1998.

[66] Dan Chen, Pat Morin, and Uli Wagner. Absolute approximation of tukey depth: Theory and experiments. *Computational Geometry*, 46(5):566 – 573, 2013.

[67] Pavlo Mozharovskyi, Karl Mosler, and Tatjana Lange. Classifying real-world data with the $DD\alpha$ -procedure. *Advances in Data Analysis and Classification*, 9(3):287–314, 2015.

[68] François-Pierre Paty and Marco Cuturi. Subspace robust Wasserstein distances. In *Proceedings of the 36th International Conference on Machine Learning*, volume 97, pages 5072–5081, 2019.

[69] Debarghya Mukherjee, Aritra Guha, Justin Solomon, Yuekai Sun, and Mikhail Yurochkin. Outlier-robust optimal transport, 2020. preprint arXiv:2012.07363.

[70] Yogesh Balaji, Rama Chellappa, and Soheil Feizi. Robust optimal transport with applications in generative modeling and domain adaptation, 2020. preprint arXiv:2010.05862.

[71] Lénaïc Chizat, Gabriel Peyré, Bernhard Schmitzer, and François-Xavier Vialard. *Journal of Functional Analysis*, 274(11):3090 – 3123, 2018.

[72] Guillaume Staerman, Pierre Laforgue, Pavlo Mozharovskyi, and Florence d’Alché Buc. When ot meets mom: Robust estimation of wasserstein distance. In *Proceedings of The 24th International Conference on Artificial Intelligence and Statistics*, volume 130, pages 136–144, 2021.

[73] Guillaume Lecué and Matthieu Lerasle. Robust machine learning by median-of-means: Theory and practice. *Ann. Statist.*, 48(2):906–931, 04 2020.

[74] Pierre Laforgue, Guillaume Staerman, and Stéphan Cléménçon. Generalization bounds in the presence of outliers: a median-of-means study. arxiv.org/abs/2006.05240, 2020.

[75] Aden Forrow, Jan-Christian Hüttner, Mor Nitzan, Philippe Rigollet, Geoffrey Schiebinger, and Jonathan Weed. Statistical optimal transport via factored couplings. In *AISTATS*, pages 2454–2465, 2019.

[76] F. Pedregosa, G. Varoquaux, A. Gramfort, V. Michel, B. Thirion, O. Grisel, M. Blondel, P. Prettenhofer, R. Weiss, V. Dubourg, J. Vanderplas, A. Passos, D. Cournapeau, M. Brucher, M. Perrot, and E. Duchesnay. Scikit-learn: Machine learning in Python. *Journal of Machine Learning Research*, 12:2825–2830, 2011.

[77] J. Shi and J. Malik. Normalized cuts and image segmentation. *IEEE Transactions on Pattern Analysis & Machine Intelligence*, 22(08):888–905, 2000.

[78] Tony Jebara. Images as bags of pixels. In *Computer Vision, IEEE International Conference on*, volume 2, page 265, 2003.

[79] Arthur Gretton, Karsten Borgwardt, Malte Rasch, Bernhard Schölkopf, and Alex Smola. A kernel method for the two-sample-problem. In B. Schölkopf, J. Platt, and T. Hoffman, editors, *Advances in Neural Information Processing Systems*, volume 19. MIT Press, 2007.

[80] C. E. Shannon. A mathematical theory of communication. *The Bell System Technical Journal*, 27(3):379–423, 1948.

[81] Lawrence Hubert and Phipps Arabie. Comparing partitions. *Journal of Classification*, 2(1):193–218, 1985.

[82] Alicia Nieto-Reyes and Heather Battey. A topologically valid definition of depth for functional data. *Statistical Science*, 31(1):61–79, 2016. Correction to this article: *Statistical Science* **32** (2017) p. 640.

[83] Christophe Ley, Camille Sabbah, and Thomas Verdebout. A new concept of quantiles for directional data and the angular Mahalanobis depth. *Electronic Journal of Statistics*, 8(1):795–816, 2014.

[84] Davy Paindaveine and Germain Van Bever. Halfspace depths for scatter, concentration and shape matrices. *The Annals of Statistics*, 46(6B):3276–3307, 12 2018.

[85] Pierre Lafaye de Micheaux, Pavlo Mozharovskyi, and Myriam Vimond. Depth for curve data and applications. *Journal of the American Statistical Association*, pages 1–17, 2020. in press.

[86] Ignacio Cascos, Qiyu Li, and Ilya Molchanov. Depth and outliers for samples of sets and random sets distributions. *Australian & New Zealand Journal of Statistics*, 2021. in press.

[87] Eddie Aamari, Ery Arias-Castro, and Clément Berenfeld. From graph centrality to data depth, 2021. preprint arXiv: 2105.03122.

[88] Rainer Dyckerhoff. Convergence of depths and depth-trimmed regions. *arXiv preprint arXiv:1611.08721*, 2017.

[89] Han Xiao, Kashif Rasul, and Roland Vollgraf. Fashion-mnist: a novel image dataset for benchmarking machine learning algorithms, 2017.

[90] Tomas Mikolov, Edouard Grave, Piotr Bojanowski, Christian Puhrsch, and Armand Joulin. Advances in pre-training distributed word representations. In *Proceedings of the Eleventh International Conference on Language Resources and Evaluation (LREC 2018)*, May 2018.

Supplementary Material

This supplementary material is organized as follows:

- Appendix A contains additional notations as well as useful preliminary results.
- Appendix B contains the proofs of the propositions/theorems provided in the paper.
- Appendix C contains approximation algorithms to compute halfspace/projection depth.
- Appendix D contains additional experiments.

A Preliminary Results

First, we introduce additional notations and recall some lemmas, used in the subsequent proofs.

A.1 Hausdorff Distance

The Hausdorff distance between two subspaces $\mathcal{K}_1, \mathcal{K}_2$ of \mathbb{R}^d is defined as

$$d_{\mathcal{H}}(\mathcal{K}_1, \mathcal{K}_2) = \max \left\{ \sup_{x \in \mathcal{K}_1} \inf_{y \in \mathcal{K}_2} \|x - y\|, \sup_{y \in \mathcal{K}_2} \inf_{x \in \mathcal{K}_1} \|x - y\| \right\}.$$

Furthermore, if \mathcal{K}_1 and \mathcal{K}_2 are convex bodies (*i.e.* non empty compact convex sets), the Hausdorff distance can be reformulated with support functions of $\mathcal{K}_1, \mathcal{K}_2$:

$$d_{\mathcal{H}}(\mathcal{K}_1, \mathcal{K}_2) = \sup_{u \in \mathbb{S}^{d-1}} |h_{\mathcal{K}_1}(u) - h_{\mathcal{K}_2}(u)|,$$

where $h_{\mathcal{K}_1}(u) = \sup\{\langle u, x \rangle, x \in \mathcal{K}_1\}$.

A.2 Depth-Trimmed Regions

Let $u \in \mathbb{S}^{d-1}$ and $X \sim \mu$ where $\mu \in \mathcal{M}_1(\mathcal{X})$ with $\mathcal{X} \subset \mathbb{R}^d$. We define the $(1 - \alpha)$ directional quantile of a distribution μ in the direction u as

$$q_{\mu, u}^{1-\alpha} = \inf \{t \in \mathbb{R} : \mathbb{P}(\langle u, X \rangle \leq t) \geq 1 - \alpha\} \quad (7)$$

and the upper $(1 - \alpha)$ quantile set of μ

$$Q_{\mu, u}^{1-\alpha} = \{x \in \mathbb{R}^d : \langle u, x \rangle \leq q_{\mu, u}^{1-\alpha}, \forall u \in \mathbb{S}^{d-1}\}. \quad (8)$$

A.3 Auxiliary Results

We now recall useful results, so as to characterize the halfspace depth regions.

Lemma 1 ([58], lemma 1). *Let $\mu \in \mathcal{M}_1(\mathcal{X})$, for any $\alpha \in (0, 1)$, it holds: $D_{\mu}^{\alpha} = Q_{\mu, u}^{1-\alpha}$.*

Lemma 2 ([58], proposition 1). *Let $\mu \in \mathcal{M}_1(\mathcal{X})$ with a $(1 - \alpha)$ directional quantile $q_{\mu, u}^{1-\alpha}$. Assume that $u \mapsto q_{\mu, u}^{1-\alpha}$ are sublinear, *i.e.*, $q_{\mu, u+\lambda v}^{1-\alpha} \leq q_{\mu, u}^{1-\alpha} + \lambda q_{\mu, v}^{1-\alpha}$, $\forall \lambda > 0$. Then for any $u \in \mathbb{S}^{d-1}$, it holds $h_{Q_{\mu, u}^{1-\alpha}}(u) = q_{\mu, u}^{1-\alpha}$.*

Lemma 3 ([58], lemma 7). *Let $u \mapsto q_{\mu, u}^{1-\alpha}$ be continuous on \mathbb{S}^{d-1} for any $\alpha \in (0, 1)$. Let $\alpha, \alpha' \in (0, 1)$ and $R > r > 0$ such that $B(0, r) \subset D_{\mu}^{\alpha} \subset B(0, R)$. Define $\omega = \max_{u \in \mathbb{S}^{d-1}} |q_{\mu, u}^{1-\alpha'} - q_{\mu, u}^{1-\alpha}|$. If $\omega < r$, it holds:*

$$d_{\mathcal{H}}(D_{\mu}^{\alpha'}, D_{\mu}^{\alpha}) \leq \frac{\omega R}{r} \frac{1 + \omega/r}{1 - \omega/r}. \quad (9)$$

Theorem 2 ([58], theorem 2). *Let $\tau, r, R > 0$ such that $\tau < r < R$. Assume that the following hypotheses are satisfied:*

- For all $u \in \mathbb{S}^{d-1}$, the cdf F_u of $\langle u, X \rangle$ is continuous on $[q_{\mu,u}^{1-\alpha} - \tau, q_{\mu,u}^{1-\alpha} + \tau]$.
- $F_u(q) - F_u(q_{\mu,u}^{1-\alpha}) \geq L(q - q_{\mu,u}^{1-\alpha})$, for all $u \in \mathbb{S}^{d-1}$ and all $q \in \mathbb{R}$ with $q_{\mu,u}^{1-\alpha} - \tau \leq q \leq q_{\mu,u}^{1-\alpha} + \tau$.
- There exists $a \in \mathbb{R}^d$ such that $B(a, r) \subset D_\mu^\alpha \subset B(a, R)$.

Then, it holds:

$$\mathbb{P} \left(d_{\mathcal{H}}(D_\mu^\alpha, D_{\mu_n}^\alpha) > \frac{Cx}{\sqrt{n}} \right) \leq A \exp^{-L^2 x^2 / 2 + 10x \sqrt{5(d+1)}},$$

for all $x \geq 0$ with $\frac{10\sqrt{5(d+1)}}{L} \leq x < \tau\sqrt{n}$, where $C = \frac{R}{r} \frac{1+\tau/r}{1-\tau/r}$ and $A = e^{-250(d+1)}$.

In order to recall two general lemmas characterizing the consistency of data depth and data depth regions, we first introduce a useful definition of strict monotonicity of a data depth.

Definition 2. Let $\mu \in \mathcal{M}_1(\mathcal{X})$. A data depth D is said strictly monotone in μ if for any $\alpha \in (0, \alpha_{\max}(\mu))$ we have

$$D_\mu^\alpha = \text{cl}\{z \in \mathbb{R}^d, D_\mu(z) > \alpha\},$$

where $\text{cl}(\mathcal{K})$ is the closure of a set \mathcal{K} .

Lemma 4 ([88], theorem 3.2). For any $\alpha \in (0, \alpha_{\max}(\mu))$ The mapping $\alpha \mapsto D_\mu^\alpha$ is continuous w.r.t. the Hausdorff distance if and only if the convex depth D is strictly monotone for μ .

Lemma 5 ([88], theorem 4.5). If the convex data depth function D is strictly monotone for μ then $\sup_{x \in \mathbb{R}^d} |D_{\hat{\mu}_n}(x) - D_\mu| \xrightarrow{a.s} 0$ implies $\sup_{\alpha \in (0, \alpha_{\max}(\mu))} d_{\mathcal{H}}(D_{\hat{\mu}_n}^\alpha, D_\mu^\alpha) \xrightarrow{a.s} 0$.

B Technical Proofs

We now prove the main results stated in the paper.

B.1 Proof of Proposition 1

For any $\alpha^* \geq \alpha \geq \varepsilon$ with $\varepsilon > 0$, and any $\mu \in \mathcal{M}_1(\mathcal{X})$, $\nu \in \mathcal{M}_1(\mathcal{Y})$, $D_\mu^\alpha, D_\nu^\alpha$ are non-empty compact subsets of \mathbb{R}^d due to the properties D2-D3. The Hausdorff distance $d_{\mathcal{H}}$, recalled in Section A.1, is known to be a distance on the space of non-empty compact sets which implies that $DR_{p,\varepsilon}$ satisfies positivity and symmetry. Triangle inequality holds thanks to Minkowski inequality. If $\mu = \nu$ then $D_\mu^\alpha = D_\nu^\alpha$, $\forall \alpha^* \geq \alpha \geq \varepsilon$ which leads to $DR_{p,\varepsilon}(\mu, \nu) = 0$. The reverse is not true. Indeed, $DR_{p,\varepsilon}(\mu, \nu) = 0$ implies $D_\mu^\alpha = D_\nu^\alpha$, $\forall \alpha^* \geq \alpha \geq \varepsilon$. Thus, $DR_{p,\varepsilon}$ is a distance if and only if the upper level sets of the chosen data depth characterize the distribution.

B.2 Proof of Proposition 2

Let $A \in \mathbb{R}^{d \times d}$ be a non singular matrix and $b \in \mathbb{R}^d$ such that $g : x \mapsto Ax + b$. Then, it holds:

$$\begin{aligned} (\alpha^* - \varepsilon) DR_{p,\varepsilon}^p(g_\sharp \mu, g_\sharp \nu) &= \int_{\varepsilon}^{\alpha^*} \left[d_{\mathcal{H}}(D_{g_\sharp \mu}^\alpha, D_{g_\sharp \nu}^\alpha) \right]^p d\alpha \\ &\stackrel{(ii)}{=} \int_{\varepsilon}^{\alpha^*} \left[d_{\mathcal{H}}(AD_\mu^\alpha + b, AD_\nu^\alpha + b) \right]^p d\alpha, \end{aligned} \quad (10)$$

where (ii) holds because any data depth satisfies (D1) by definition. Furthermore,

$$\begin{aligned}
d_{\mathcal{H}}(AD_{\mu}^{\alpha} + b, AD_{\nu}^{\alpha} + b) &= \max \left\{ \sup_{x \in D_{\mu}^{\alpha}} \inf_{y \in D_{\nu}^{\alpha}} \|Ax - Ay\|, \sup_{y \in D_{\nu}^{\alpha}} \inf_{x \in D_{\mu}^{\alpha}} \|Ax - Ay\| \right\} \\
&\stackrel{(iii)}{=} \max \left\{ \sup_{x \in D_{\mu}^{\alpha}} \inf_{y \in D_{\nu}^{\alpha}} \|x - y\|, \sup_{y \in D_{\nu}^{\alpha}} \inf_{x \in D_{\mu}^{\alpha}} \|x - y\| \right\} \\
&= d_{\mathcal{H}}(D_{\mu}^{\alpha}, D_{\nu}^{\alpha}),
\end{aligned}$$

where (iii) holds by virtue of hypothesis $AA^{\top} = I_d$. Replacing it in (10) yields the desired results.

B.3 Proof of Proposition 3

First assertion. Denote Z_1, Z_2 two random variables following μ^*, ν^* respectively. For any $x \in \mathbb{R}^d$ and $\alpha \in [0, 1]$,

$$\begin{aligned}
x \in D_{\mu}^{\alpha} &\iff HD_{\mu}(x) \geq \alpha \iff \forall u \in \mathbb{R}^d \mathbb{P}(\langle u, X \rangle \leq \langle u, x \rangle) \geq \alpha \\
&\iff \forall u \in \mathbb{R}^d \mathbb{P}(\langle u, Z_1 + \mathbf{m}_1 \rangle \leq \langle u, x \rangle) \geq \alpha \\
&\iff \forall u \in \mathbb{R}^d \mathbb{P}(\langle u, Z_1 \rangle \leq \langle u, x - \mathbf{m}_1 \rangle) \geq \alpha \\
&\iff x - \mathbf{m}_1 \in D_{\mu^*}^{\alpha}
\end{aligned}$$

The same reasoning holds for ν and ν^* . Following this, for any $\alpha \in [0, 1]$ and $u \in \mathbb{S}^{d-1}$, it holds

$$h_{D_{\mu}^{\alpha}}(u) = h_{D_{\mu^*}^{\alpha}}(u) - \langle u, \mathbf{m}_1 \rangle \quad \text{and} \quad h_{D_{\nu}^{\alpha}}(u) = h_{D_{\nu^*}^{\alpha}}(u) - \langle u, \mathbf{m}_2 \rangle$$

Thus it holds

$$\begin{aligned}
DR_{2,\varepsilon}^2(\mu, \nu) &= \frac{1}{\alpha^* - \varepsilon} \int_{\varepsilon}^{\alpha^*} \sup_{u \in \mathbb{S}^{d-1}} \left| h_{D_{\mu^*}^{\alpha}}(u) - \langle u, \mathbf{m}_1 \rangle - h_{D_{\nu^*}^{\alpha}}(u) + \langle u, \mathbf{m}_2 \rangle \right|^2 d\alpha \\
&\leq \sup_{u \in \mathbb{S}^{d-1}} |\langle u, \mathbf{m}_1 - \mathbf{m}_2 \rangle|^2 + \frac{1}{\alpha^* - \varepsilon} \int_{\varepsilon}^{\alpha^*} \sup_{u \in \mathbb{S}^{d-1}} |h_{D_{\mu^*}^{\alpha}}(u) - h_{D_{\nu^*}^{\alpha}}(u)|^2 d\alpha \\
&\quad + 2 \sup_{u \in \mathbb{S}^{d-1}} |\langle u, \mathbf{m}_1 - \mathbf{m}_2 \rangle| \frac{1}{\alpha^* - \varepsilon} \int_{\varepsilon}^{\alpha^*} \sup_{u \in \mathbb{S}^{d-1}} |h_{D_{\mu^*}^{\alpha}}(u) - h_{D_{\nu^*}^{\alpha}}(u)| d\alpha \\
&= \|\mathbf{m}_1 - \mathbf{m}_2\|^2 + DR_{2,\varepsilon}^2(\mu^*, \nu^*) + 2\|\mathbf{m}_1 - \mathbf{m}_2\|DR_{1,\varepsilon}(\mu^*, \nu^*). \tag{11}
\end{aligned}$$

On the other side we have

$$\begin{aligned}
DR_{2,\varepsilon}^2(\mu, \nu) &\geq \sup_{u \in \mathbb{S}^{d-1}} |\langle u, \mathbf{m}_1 - \mathbf{m}_2 \rangle|^2 + \frac{1}{\alpha^* - \varepsilon} \int_{\varepsilon}^{\alpha^*} \sup_{u \in \mathbb{S}^{d-1}} |h_{D_{\mu^*}^{\alpha}}(u) - h_{D_{\nu^*}^{\alpha}}(u)|^2 d\alpha \\
&\quad - 2 \sup_{u \in \mathbb{S}^{d-1}} |\langle u, \mathbf{m}_1 - \mathbf{m}_2 \rangle| \frac{1}{\alpha^* - \varepsilon} \int_{\varepsilon}^{\alpha^*} \sup_{u \in \mathbb{S}^{d-1}} |h_{D_{\mu^*}^{\alpha}}(u) - h_{D_{\nu^*}^{\alpha}}(u)| d\alpha \\
&= \|\mathbf{m}_1 - \mathbf{m}_2\|^2 + DR_{2,\varepsilon}^2(\mu^*, \nu^*) - 2\|\mathbf{m}_1 - \mathbf{m}_2\|DR_{1,\varepsilon}(\mu^*, \nu^*). \tag{12}
\end{aligned}$$

Combining (11) and (12) leads to the desired result.

Second assertion. For any $u \in \mathbb{S}^{d-1}$, the $(1 - \alpha)$ quantile of random variables $\langle u, X \rangle$ and $\langle u, Y \rangle$ such that $\langle u, X \rangle \sim \mathcal{N}(\langle u, \mathbf{m}_1 \rangle, u^{\top} \Sigma_1 u)$ and $\langle u, Y \rangle \sim \mathcal{N}(\langle u, \mathbf{m}_2 \rangle, u^{\top} \Sigma_2 u)$ are defined by

$$q_{\mu,u}^{1-\alpha} = \langle u, \mathbf{m}_1 \rangle + \Phi^{-1}(1 - \alpha) \sqrt{u^{\top} \Sigma_1 u} \quad q_{\nu,u}^{1-\alpha} = \langle u, \mathbf{m}_2 \rangle + \Phi^{-1}(1 - \alpha) \sqrt{u^{\top} \Sigma_2 u},$$

where Φ is the cumulative distribution function of the univariate standard Gaussian distribution.

Now, to apply Lemma 2, it is sufficient to prove that directional quantiles are sublinear. It holds using subadditivity of the square root function. Indeed, for any $u, v \in \mathbb{S}^{d-1}$ and $\lambda > 0$, we have:

$$\begin{aligned}
& \langle u + \lambda v, \mathbf{m}_1 \rangle + \Phi^{-1}(1 - \alpha) \sqrt{(u + \lambda v)^\top \Sigma_1 (u + \lambda v)} \\
&= \langle u, \mathbf{m}_1 \rangle + \lambda \langle v, \mathbf{m}_1 \rangle + \Phi^{-1}(1 - \alpha) \sqrt{(u + \lambda v)^\top \Sigma_1 (u + \lambda v)} \\
&\leq \langle u, \mathbf{m}_1 \rangle + \lambda \langle v, \mathbf{m}_1 \rangle + \Phi^{-1}(1 - \alpha) \left[\sqrt{u^\top \Sigma_1 u} + \lambda \sqrt{v^\top \Sigma_1 v} \right] \\
&= q_{\mu, u}^{1-\alpha} + \lambda q_{\mu, v}^{1-\alpha}.
\end{aligned}$$

The same reasoning holds for ν . Applying Lemma 1 and Lemma 2, for any $u \in \mathbb{S}^{d-1}$, we have $h_{D_\mu^\alpha}(u) = q_{\mu, u}^{1-\alpha}$ and $h_{D_\nu^\alpha}(u) = q_{\nu, u}^{1-\alpha}$. It follows:

$$\begin{aligned}
DR_{1, \varepsilon}(\mu, \nu) &= \frac{1}{\alpha^* - \varepsilon} \int_\varepsilon^{\alpha^*} d_{\mathcal{H}}(D_\mu^\alpha, D_\nu^\alpha) d\alpha = \frac{1}{\alpha^* - \varepsilon} \int_\varepsilon^{\alpha^*} \sup_{u \in \mathbb{S}^{d-1}} |h_{D_\mu^\alpha}(u) - h_{D_\nu^\alpha}(u)| d\alpha \\
&= \frac{1}{\alpha^* - \varepsilon} \int_\varepsilon^{\alpha^*} \sup_{u \in \mathbb{S}^{d-1}} \left| \langle u, \mathbf{m}_1 - \mathbf{m}_2 \rangle + \Phi^{-1}(1 - \alpha) \left[\sqrt{u^\top \Sigma_1 u} - \sqrt{u^\top \Sigma_2 u} \right] \right| d\alpha \\
&\leq \|\mathbf{m}_1 - \mathbf{m}_2\| + \frac{1}{\alpha^* - \varepsilon} \int_\varepsilon^{\alpha^*} \sup_{u \in \mathbb{S}^{d-1}} \left| \Phi^{-1}(1 - \alpha) \left[\sqrt{u^\top \Sigma_1 u} - \sqrt{u^\top \Sigma_2 u} \right] \right| d\alpha \\
&= \|\mathbf{m}_1 - \mathbf{m}_2\| + C_\varepsilon \sup_{u \in \mathbb{S}^{d-1}} \left| \sqrt{u^\top \Sigma_1 u} - \sqrt{u^\top \Sigma_2 u} \right|,
\end{aligned}$$

with $C_\varepsilon = \frac{1}{\alpha^* - \varepsilon} \int_\varepsilon^{\alpha^*} |\Phi^{-1}(1 - \alpha)| d\alpha$.

The lower bound is obtained by means the same reasoning. Notice that

$$\|\mathbf{m}_1 - \mathbf{m}_2\| = \sup_{u \in \mathbb{S}^{d-1}} |\langle u, \mathbf{m}_1 - \mathbf{m}_2 \rangle| = \frac{1}{\alpha^* - \varepsilon} \int_\varepsilon^{\alpha^*} \sup_{u \in \mathbb{S}^{d-1}} |\langle u, \mathbf{m}_1 - \mathbf{m}_2 \rangle| d\alpha.$$

Introducing $h_{D_\mu^\alpha}(u), h_{D_\nu^\alpha}(u)$ and using triangular inequality, subadditivity of the supremum and linearity of the integral, we obtain:

$$\|\mathbf{m}_1 - \mathbf{m}_2\| \leq DR_{1, \varepsilon}(\mu, \nu) + C_\varepsilon \sup_{u \in \mathbb{S}^{d-1}} \left| \sqrt{u^\top \Sigma_1 u} - \sqrt{u^\top \Sigma_2 u} \right|,$$

which ends the proof.

B.4 Proof of Proposition 4

We have

$$\begin{aligned}
DR_{p, \varepsilon}^p(\hat{\mu}_n, \mu) &= \frac{1}{\alpha^* - \varepsilon} \int_\varepsilon^{\alpha^*} [d_{\mathcal{H}}(D_{\hat{\mu}_n}^\alpha, D_\mu^\alpha)]^p d\alpha \leq \sup_{\alpha \in [\varepsilon, \alpha^*]} [d_{\mathcal{H}}(D_{\hat{\mu}_n}^\alpha, D_\mu^\alpha)]^p \\
&\leq \sup_{\alpha \in [\varepsilon, \alpha_{\max}(\mu)]} [d_{\mathcal{H}}(D_{\hat{\mu}_n}^\alpha, D_\mu^\alpha)]^p.
\end{aligned}$$

Now, if $\alpha \mapsto D_\mu^\alpha$ is a continuous function w.r.t. the Hausdorff distance and $D_{\hat{\mu}_n}$ converges uniformly to D_μ , using continuity of $x \mapsto x^p$ and applying lemma 4 and 5 lead to the desired result.

B.5 Proof of Theorem 1

We now prove a non-asymptotic bound of the proposed pseudo-metric $DR_{p,\varepsilon}$ associated with the halfspace depth. This proof is a slight adaptation of the proof of Theorem 2, extending the latter to the uniform case. First, notice that, for any $z > 0$,

$$\mathbb{P}(DR_{\varepsilon,p}^-(\mu_n, \mu) > z) \leq \mathbb{P}\left(\sup_{\alpha \in [\varepsilon, \alpha^* - \varepsilon]} d_{\mathcal{H}}(D_{\mu_n}^\alpha, D_\mu^\alpha) > z\right).$$

Let α be in $\mathcal{I}_\varepsilon := [\varepsilon, \alpha^* - \varepsilon]$ with $\varepsilon > 0$. Let \mathcal{A} be the event $\mathcal{A} = \{|\hat{q}_u^{1-\alpha} - q_u^{1-\alpha}| \leq y, \forall u \in \mathbb{S}^{d-1}, \forall \alpha \in \mathcal{I}_\varepsilon\}$ with $y \in [10\sqrt{5(d+1)}/(L\sqrt{n}), \gamma]$. D_μ^α is a convex body for every $\alpha \in \mathcal{I}_\varepsilon$, then there exists $a_\alpha, r_\alpha, R_\alpha$ positive numbers such that $B(a_\alpha, r_\alpha) \subset D_\mu^\alpha \subset B(a_\alpha, R_\alpha)$. Therefore, $r_\alpha = \langle u, r_\alpha u \rangle \leq q_u^{1-\alpha}$ for any $\alpha \in \mathcal{I}_\varepsilon$ and $u \in \mathbb{S}^{d-1}$. It follows that $\hat{q}_u^{1-\alpha} \geq q_u^{1-\alpha} - y \geq r_\alpha - \gamma > 0$ which implies that $B(a_\alpha, r_\alpha - \gamma) \subset D_{\mu_n}^\alpha$. By virtue of Lemma 12 and Lemma 16 in [58], for any $\alpha \in \mathcal{I}_\varepsilon$, the mappings $u \mapsto q_u^{1-\alpha}$ and $u \mapsto \hat{q}_u^{1-\alpha}$ are continuous. Thus, it follows from Lemma 7 in [58] and the fact that the function $x \mapsto (1+x)/(1-x)$ is nondecreasing on $[0, 1)$, that: $\forall \alpha \in \mathcal{I}_\varepsilon$,

$$d_{\mathcal{H}}(D_{\mu_n}^\alpha, D_\mu^\alpha) \leq \frac{yR_\alpha}{r_\alpha} \frac{1+y/r_\alpha}{1-y/r_\alpha} \leq c_\alpha y \leq \sup_{\alpha \in \mathcal{I}_\varepsilon} c_\alpha y,$$

with $c_\alpha = \frac{R_\alpha}{r_\alpha} \frac{1+\gamma/r_\alpha}{1-\gamma/r_\alpha}$. Hence, we have

$$\mathbb{P}\left(\sup_{\alpha \in \mathcal{I}_\varepsilon} d_{\mathcal{H}}(D_{\mu_n}^\alpha, D_\mu^\alpha) > \sup_{\alpha \in \mathcal{I}_\varepsilon} c_\alpha y\right) \leq \mathbb{P}(\mathcal{A}^c), \quad (13)$$

where \mathcal{A}^c stands for the complementary of the event \mathcal{A} . The proof of the Lemma 15 of [58] can be adapted to the uniform (in α) case using $\mathcal{C}_0 = \{(u, s) \in \mathbb{S}^{d-1} \times \mathbb{R} : q_u^\varepsilon - \gamma \leq s \leq q_u^{\alpha^* - \varepsilon} + \gamma\}$ which allows us to bound $\mathbb{P}(\mathcal{A}^c)$. Thus, taking $y = t/\sqrt{n}$, such that $\frac{10\sqrt{5(d+1)}}{L} \leq t \leq \gamma\sqrt{n}$ leads to

$$\mathbb{P}(\mathcal{A}^c) \leq e^{-250(d+1)} \exp\left(-L^2 t^2/2 + 10Lt\sqrt{5(d+1)}\right). \quad (14)$$

Following (13) and (14) lead to

$$\mathbb{P}\left(\sup_{\alpha \in \mathcal{I}_\varepsilon} d_{\mathcal{H}}(D_{\mu_n}^\alpha, D_\mu^\alpha) > \sup_{\alpha \in \mathcal{I}_\varepsilon} c_\alpha t/\sqrt{n}\right) \leq e^{-250(d+1)} \exp\left(-L^2 t^2/2 + 10Lt\sqrt{5(d+1)}\right),$$

which proves the desired result.

B.6 Proof of Proposition 5

For $DR_{p,\varepsilon}$ to break down at \mathcal{S}_n , it needs to have at least one trimmed-region that breaks down. Then the break downpoint of $DR_{p,\varepsilon}$ is higher than the minimum of the breakdown point of each region. Indeed we have

$$\begin{aligned} BP(DR_{p,\varepsilon}, \mathcal{S}_n) &= \min \left\{ \frac{o}{n+o} : \sup_{Z_1, \dots, Z_o} DR_{p,\varepsilon}(\hat{\mu}_{n+o}, \hat{\mu}_n) = +\infty \right\} \\ &\geq \min_{\alpha \in [\varepsilon, \hat{\alpha}^*]} \min \left\{ \frac{o}{n+o} : \sup_{Z_1, \dots, Z_o} d_{\mathcal{H}}(D_{\mu_n+o}^\alpha, D_{\mu_n}^\alpha) = +\infty \right\} \\ &= \min_{\alpha \in [\varepsilon, \hat{\alpha}^*]} BP(D_{\mu_n}^\alpha, \mathcal{S}_n), \end{aligned}$$

where $\hat{\alpha}^* = \alpha_{\max}(\hat{\mu}_{n+o}) \wedge \alpha_{\max}(\hat{\mu}_n)$. Now applying Lemma 3.1 in [48] and Theorem 4 in [61], a lower bound of the breakdown point of each halfspace region, for every $\alpha \in (0, \alpha_{\max}(\hat{\mu}_n))$, is given by

$$BP(D_{\hat{\mu}_n}^\alpha, \mathcal{S}_n) \geq \begin{cases} \frac{\lceil n\alpha/(1-\alpha) \rceil}{n + \lceil n\alpha/(1-\alpha) \rceil} & \text{if } \alpha \leq \frac{\alpha_{\max}(\hat{\mu}_n)}{1 + \alpha_{\max}(\hat{\mu}_n)}, \\ \frac{\alpha_{\max}(\hat{\mu}_n)}{1 + \alpha_{\max}(\hat{\mu}_n)} & \text{otherwise,} \end{cases}$$

which leads to the result.

C Approximation Algorithms

In this part, we display the approximation algorithms of the halfspace depth (see Algorithm 2) and the projection depth (see Algorithm 3) used in the first step of the Algorithm 1 of the paper.

Algorithm 2 Approximation of the halfspace depth

Initialization: K .

- 1: Construct $\mathbf{U} \in \mathbb{R}^{d \times K}$ by sampling uniformly K vectors U_1, \dots, U_K in \mathbb{S}^{d-1}
- 2: Compute $\mathbf{M} = \mathbf{XU}$
- 3: Compute the rank value $\sigma(i, k)$, the rank of index i in $\mathbf{M}_{:,k}$ for every $i \leq n$ and $k \leq K$
- 4: Set $D_i = \min_{k \leq K} \sigma(i, k)$ for every $i \leq n$

Output: D, \mathbf{M}

Algorithm 3 Approximation of the projection depth

Initialization: K .

- 1: Construct $\mathbf{U} \in \mathbb{R}^{d \times K}$ by sampling uniformly K vectors U_1, \dots, U_K in \mathbb{S}^{d-1}
- 2: Compute $\mathbf{M} = \mathbf{XU}$
- 3: Find $\mathbf{M}_{\text{med},k}$ the median value of $\mathbf{M}_{:,k}$, $\forall k \leq K$
- 4: Compute $\text{MAD}_k = \text{median}\{|\mathbf{M}_{i,k} - \mathbf{M}_{\text{med},k}|, i \leq n\}$ for $k \leq K$
- 5: Compute \mathbf{V} s.t. $\mathbf{V}_{i,k} = |\mathbf{M}_{i,k} - \mathbf{M}_{\text{med},k}|/\text{MAD}_k$
- 6: Set $D_i = \min_{k \leq K} 1/(1 + \mathbf{V}_{i,k})$ for every $i \leq n$

Output: D, \mathbf{M}

D Additional Experiments

D.1 Illustration of Data Depth Contours

Figure 3, which plots a family of halfspace depth induced trimmed regions for a data set contaminated with outliers, illustrates the robustness.

D.2 The choice of the parameter n_α

Proposition 3 allows to derive a closed form expression for $DR_{2,\varepsilon}(\mu, \nu)$ when μ, ν are Gaussian distributions with the same variance-covariance matrix. In order to investigate the quality of the approximation on light-tailed and heavy-tailed distributions, we focus on computing $DR_{2,0.1}$ (with $K = 500$) for varying number of n_α between a sample of 1000 points stemming from $\mu \sim \mathcal{N}(\mathbf{0}_d, \Sigma)$ for $d \in \{2, 3, 10\}$, Σ drawn uniformly from the space of positive matrices and three different samples (which yields nine settings). These three samples are constructed from 1000 observations stemming from *Gaussian*, *Student-t₂* and *Cauchy* distributions all with an expectation equal to $\mathbf{7}_d$. Results, that report the averaged approximation error as well as the 25-75% empirical quantile intervals are depicted in Figure 4. They show that $DR_{p,\varepsilon}$ converges slowly for *Cauchy* and *Student-t₂* with growing n_α , while it converges with small n_α for *Gaussian* distribution.

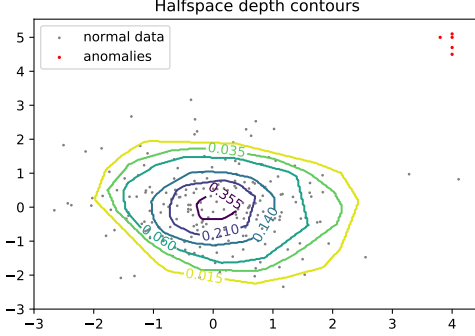


Figure 3: Halfspace depth contours for a bivariate sample contaminated with outliers.

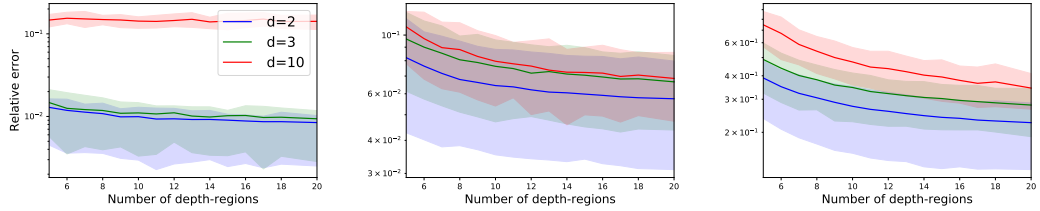


Figure 4: Relative approximation error (averaged over 100 repetitions) of $DR_{p,\varepsilon}$ for *Gaussian* (left), *Student-t₂* (middle) and *Cauchy* (right) distributions for differing numbers of n_α .

D.3 Robustness to outliers

Datasets on which experiments about "Robustness to outliers" in Section 5 have been performed are displayed in Figure 5.

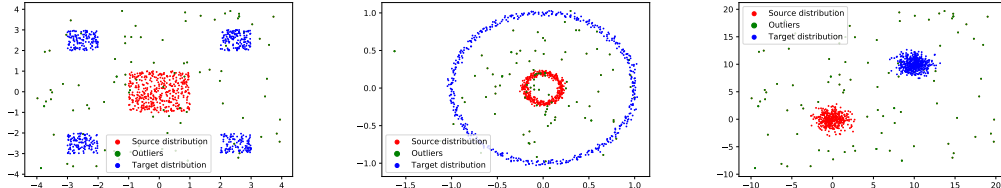


Figure 5: Datasets related to robustness experiments depicted in Section 5 with 20% of outliers for *fragmented hypercube* (left), *circles* (middle) and *Gaussian* datasets (right).

D.4 Benchmarking on real-world datasets

Next, we check the relevance of the proposed pseudo-metric on two large-scale real-world data sets, namely *Fashion-MNIST* [89] and *Movies* [90]. While *Fashion-MNIST* consists of 10 classes each containing 6000 observations in dimension 784, the *Movies* data set consists of word2vec embedding in \mathbb{R}^{300} of the 7 movies scripts totaling from 746 to 1981 observations per movie. We consider pair of classes and compute (pseudo)metrics between classes seen as empirical distributions. Table 3 indicates $DR_{p,\varepsilon}$ between each pair of classes. One observes that contextually similar classes, which are indicated in bold, are substantially closer to each other. Table 4 displays the results of the Sliced-Wasserstein distance on *Fashion-MNIST* datasets. This optimal-transport distance fails to recognize similarities between classes. For example, The most similar class to 'Ankle boot' returned by SW is the class 'Bag' while it should be 'Sneaker' or 'Sandal'.

	Ts	T	P	D	C	S	Sh	Sn	B	Ab
Ts	0	2.7	2.2	2.1	2.3	3.5	1.9	3.8	2.9	3.2
T	2.7	0	3.2	1.8	3.2	3.0	2.9	3.1	3.7	3.5
P	2.2	3.2	0	2.7	1.6	3.5	1.4	3.8	2.4	3.1
D	2.1	1.8	2.7	0	2.6	2.9	2.4	3.2	3.2	3.1
C	2.3	3.2	1.6	2.6	0	3.5	1.9	3.7	2.5	3.0
S	3.5	3.0	3.5	2.9	3.5	0	3.2	1.8	3.0	2.4
Sh	1.9	2.9	1.4	2.4	1.9	3.2	0	3.5	2.4	2.9
Sn	3.8	3.1	3.8	3.2	3.7	1.8	3.5	0	3.2	2.7
B	2.9	3.7	2.4	3.2	2.5	3.0	2.4	3.2	0	2.5
Ab	3.2	3.5	3.1	3.1	3.0	2.4	2.9	2.7	2.5	0

	D	G	I	KB1	KB2	TM	T
D	0	0.31	0.32	0.30	0.32	0.34	0.29
G	0.31	0	0.27	0.34	0.31	0.32	0.34
I	0.32	0.27	0	0.39	0.29	0.28	0.32
KB1	0.30	0.34	0.39	0	0.29	0.32	0.30
KB2	0.32	0.31	0.30	0.29	0	0.30	0.34
TM	0.34	0.32	0.28	0.32	0.30	0	0.32
T	0.29	0.34	0.32	0.30	0.34	0.32	0

Table 3: $DR_{p,\varepsilon}$ distance with $\varepsilon = 0, p = 2$ and $K = 10^4$ between Fashion-MNIST classes (left) and movie scripts (right). Bold values corresponds to the most similar for each of them. Fashion-MNIST classes (types of clothes): TS: T-shirt/top, T: Trouser, P: Pullover, D: Dress, C: Coat, S: Sandal, Sh: Shirt, Sn: Sneaker, B: Bag, Ab: Ankle boot. Movies: D: Dunkirk, G: Gravity, I: Interstellar, KB1: Kill Bill Vol.1, KB2: Kill Bill Vol.2, TM: The Martian, T: Titanic.

	Ts	T	P	D	C	S	Sh	Sn	B	Ab
Ts	0	0.48	0.41	0.33	0.43	0.69	0.28	0.74	0.56	0.7
T	0.48	0.	0.63	0.31	0.61	0.66	0.53	0.71	0.73	0.78
P	0.41	0.63	0	0.53	0.19	0.69	0.20	0.73	0.44	0.64
D	0.33	0.31	0.53	0	0.5	0.65	0.40	0.69	0.62	0.71
C	0.43	0.61	0.19	0.5	0	0.75	0.24	0.77	0.46	0.67
S	0.69	0.66	0.69	0.65	0.75	0	0.61	0.30	0.56	0.51
Sh	0.28	0.53	0.20	0.40	0.24	0.61	0	0.67	0.51	0.60
Sn	0.75	0.71	0.74	0.69	0.77	0.30	0.67	0	0.58	0.54
B	0.57	0.74	0.44	0.62	0.46	0.56	0.51	0.58	0	0.47
Ab	0.70	0.79	0.63	0.71	0.67	0.51	0.60	0.54	0.47	0

Table 4: The Sliced-Wasserstein distance between Fashion-MNIST classes. Bold values corresponds to the most similar for each of them. TS: T-shirt/top, T: Trouser, P: Pullover, D: Dress, C: Coat, S: Sandal, Sh: Shirt, Sn: Sneaker, B: Bag, Ab: Ankle boot.